



Contents lists available at SciVerse ScienceDirect

## Biochimica et Biophysica Acta

journal homepage: [www.elsevier.com/locate/bbadis](http://www.elsevier.com/locate/bbadis)

## Uremic toxins inhibit renal metabolic capacity through interference with glucuronidation and mitochondrial respiration

H.A.M. Mutsaers<sup>a,b</sup>, M.J.G. Wilmer<sup>a</sup>, D. Reijnders<sup>a</sup>, J. Jansen<sup>b</sup>, P.H.H. van den Broek<sup>a</sup>, M. Forkink<sup>c</sup>, E. Schepers<sup>e</sup>, G. Glorieux<sup>e</sup>, R. Vanholder<sup>e</sup>, L.P. van den Heuvel<sup>d,f</sup>, J.G. Hoenderop<sup>b</sup>, R. Masereeuw<sup>a,\*</sup>

<sup>a</sup> Department of Pharmacology and Toxicology, Radboud University Nijmegen Medical Centre, Nijmegen Centre for Molecular Life Sciences, Nijmegen, The Netherlands

<sup>b</sup> Department of Physiology, Radboud University Nijmegen Medical Centre, Nijmegen Centre for Molecular Life Sciences, Nijmegen, The Netherlands

<sup>c</sup> Department of Biochemistry, Radboud University Nijmegen Medical Centre, Nijmegen Centre for Molecular Life Sciences, Nijmegen, The Netherlands

<sup>d</sup> Department of Pediatrics, Radboud University Nijmegen Medical Centre, Nijmegen Centre for Molecular Life Sciences, Nijmegen, The Netherlands

<sup>e</sup> Renal Division, University Hospital Ghent, Ghent, Belgium

<sup>f</sup> Department of Pediatrics, Catholic University Leuven, Leuven, Belgium

## ARTICLE INFO

## Article history:

Received 16 July 2012

Received in revised form 10 September 2012

Accepted 17 September 2012

Available online 24 September 2012

## Keywords:

Uremic toxins

Chronic kidney disease

Drug metabolism

UDP-glucuronosyltransferases

Mitochondria

## ABSTRACT

During chronic kidney disease (CKD), drug metabolism is affected leading to changes in drug disposition. Furthermore, there is a progressive accumulation of uremic retention solutes due to impaired renal clearance. Here, we investigated whether uremic toxins can influence the metabolic functionality of human conditionally immortalized renal proximal tubule epithelial cells (ciPTEC) with the focus on UDP-glucuronosyltransferases (UGTs) and mitochondrial activity. Our results showed that ciPTEC express a wide variety of metabolic enzymes, including UGTs. These enzymes were functionally active as demonstrated by the glucuronidation of 7-hydroxycoumarin (7-OHC;  $K_m$  of  $12 \pm 2 \mu\text{M}$  and a  $V_{max}$  of  $76 \pm 3 \text{ pmol/min/mg}$ ) and p-cresol ( $K_m$  of  $33 \pm 13 \mu\text{M}$  and a  $V_{max}$  of  $266 \pm 25 \text{ pmol/min/mg}$ ). Furthermore, a wide variety of uremic toxins, including indole-3-acetic acid, indoxyl sulfate, phenylacetic acid and kynurenic acid, reduced 7-OHC glucuronidation with more than 30% as compared with controls ( $p < 0.05$ ), whereas UGT1A and UGT2B protein expressions remained unaltered. In addition, our results showed that several uremic toxins inhibited mitochondrial succinate dehydrogenase (*i.e.* complex II) activity with more than 20% as compared with controls ( $p < 0.05$ ). Moreover, indole-3-acetic acid decreased the reserve capacity of the electron transport system with 18% ( $p < 0.03$ ). In conclusion, this study shows that multiple uremic toxins inhibit UGT activity and mitochondrial activity in ciPTEC, thereby affecting the metabolic capacity of the kidney during CKD. This may have a significant impact on drug and uremic retention solute disposition in CKD patients.

© 2012 Elsevier B.V. All rights reserved.

## 1. Introduction

Renal function is an important aspect in drug clearance and it is widely known that drug disposition is altered in patients with chronic kidney disease (CKD) [1–3]. These changes in pharmacokinetics are partially due to a decreased glomerular filtration and tubular secretion. Another hallmark of CKD is the accumulation of potentially toxic solutes that are normally excreted *via* the urine. These uremic toxins can cause a multitude of pathologies, including renal fibrosis, anemia, bone disorders and cardio-vascular disease [4,5]. Currently, more than 110 uremic toxins are known, divided into three distinct classes based on their physico-chemical properties: the small water-soluble compounds, the middle molecules and the protein-bound solutes [5,6]. The latter group of retention solutes are actively secreted by the healthy kidney and are difficult to eliminate using current dialysis strategies [7]. Since protein-bound uremic toxins accumulate during renal failure it could be argued that these compounds affect drug metabolism in CKD patients by interacting with renal enzymes. Many drugs commonly used in the clinic are metabolized by phase II enzymes, which catalyze conjugation reactions, including sulfation, acetylation and glucuronidation [8]. Several

**Abbreviations:** 7-OHC, 7-hydroxycoumarin; 7-OHCG, 7-hydroxycoumarin glucuronide; AA, antimycin A; ciPTEC, conditionally immortalized human renal proximal tubule epithelial cells; CKD, chronic kidney disease; CMPF, 3-carboxy-4-methyl-5-propyl-2-furanpropanoic acid; CRF, chronic renal failure; CYP, cytochrome p450; E, ETS, electron transport system; FCCP, p-trifluoromethoxy carbonyl cyanide phenyl hydrazone; FCS, fetal calf serum; GST, glutathione S-transferase; HA, hippuric acid; HEK293, human embryonic kidney cells; HPLC, high-performance liquid chromatography; IA, indole-3-acetic acid; IS, indoxyl sulfate; KA, kynurenic acid; L, LEAK; M, medium; Mix, uremic toxin mix; MIT, 3-[4,5-dimethylthiazol-2-yl]-2,5-diphenyl tetrazolium bromide; NAD<sup>+</sup>, nicotinamide adenine dinucleotide; NAT, N-acetyltransferase; omy, oligomycin A; OAT, organic anion transporter; Ox, oxalate; OXPHOS, oxidative phosphorylation; pC, p-cresol; pCG, p-cresyl glucuronide; pCS, p-cresyl sulfate; PHA, phenylacetic acid; PHG, phenyl glucuronide; PHS, phenyl sulfate; PTEC, proximal tubule cells; Pu, putrescine; QA, quinolinic acid; R, ROUTINE; ROT, rotenone; ROX, residual oxygen consumption; SULT, sulfotransferase; UDPGA, UDP-glucuronic acid; UGT, UDP-glucuronosyltransferases; ZO-1, tight junction protein 1

\* Corresponding author at: Department of Pharmacology and Toxicology, Radboud University Nijmegen Medical Centre, Nijmegen Centre for Molecular Life Sciences, Geert Grooteplein 26–28, 6525 GA, Nijmegen, The Netherlands. Tel.: +31 24 3613730; fax: +31 24 3614214.

E-mail address: [r.masereeuw@pharmtox.umcn.nl](mailto:r.masereeuw@pharmtox.umcn.nl) (R. Masereeuw).

studies demonstrated that the pharmacokinetics of drugs solely cleared via phase II metabolism is changed in CKD patients. For instance, a decreased glucuronidation of metoclopramide, chloramphenicol, p-aminobenzoic acid, zidovudine and morphine have been reported in patients with chronic renal failure (CRF) [9–14]. Moreover, the acetylation of isoniazid is reduced in CKD patients [15]. However, little information is available about the mechanism underlying the observed decrease in phase II metabolism during renal failure.

UDP-glucuronosyltransferases (UGT) are an important class of phase II enzymes that catalyze the conjugation of glucuronic acid to many xenobiotics, environmental pollutants and endogenous compounds [16,17]. Next to drugs, uremic retention solutes are also prone to glucuronidation, and at least two glucuronides have been identified in uremic biological fluids, p-cresyl glucuronide and indoxyl glucuronide [18–20]. UGTs are expressed in several organs including the liver, gastro-intestinal tract and kidney, and to date 19 human UGT proteins have been identified [21,22]. Due to the relative abundance of the essential cofactor UDP-glucuronic acid (UDPGA), glucuronidation is the most prevalent conjugation reaction and under normal metabolic conditions, the supply of UDPGA is not rate-limiting for this process [23]. Yet, during excessive glycolysis or under altered redox conditions, UGT activity is impaired [23,24]. After the liver, UGT activity is highest in the kidney, emphasizing the pivotal role of this organ in facilitating xenobiotic clearance via glucuronidation [8,25]. Previously, Yu et al. demonstrated that UGT expression and activity were down-regulated in the liver and kidney of 5/6 nephrectomized rats. However, this effect was also observed in control pair-fed rats and was possibly due to a decreased food intake [26]. Thus, the repercussions of CKD on UGTs remain to be elucidated.

In the present study, conditionally immortalized human renal proximal tubule epithelial cells (ciPTEC) were used to investigate the impact of multiple uremic toxins on renal UGT activity. Our results show that ciPTEC express a broad array of drug metabolism enzymes, similar to human kidney. Furthermore, UGT proteins were functionally active in ciPTEC, as demonstrated by 7-hydroxycoumarin (7-OHC) and p-cresol glucuronidation. Uremic toxins inhibited the glucuronidation of 7-OHC without affecting UGT1A and UGT2B protein expression, indicating a reduction in enzyme activity. Moreover, exposure of ciPTEC to uremic toxins caused a reduction in mitochondrial succinate dehydrogenase activity and in the maximum capacity of the oxidative phosphorylation (OXPHOS) system, which could explain the observed inhibitory effect of uremic toxins on glucuronide formation. These results present a novel pathway via which uremic retention solutes affect the metabolic capacity of the kidney and are likely involved in altering drug metabolism by glucuronidation in CKD patients.

## 2. Materials and methods

### 2.1. Chemicals

All chemicals were obtained from Sigma (Zwijndrecht, The Netherlands) unless stated otherwise. Stock solutions of uremic toxins were prepared as described by Cohen et al., [27] and were stored at  $-20^{\circ}\text{C}$ . Both p-cresyl sulfate and phenyl sulfate were synthesized as a potassium salt as described previously [28]. P-cresyl glucuronide was produced from glucuronyl-trichloroacetimidate and p-cresol using the method previously described by Van der Eycken et al. [29].

### 2.2. Cell culture

The ciPTEC line was generated as previously described by Wilmer et al. [30]. The cells were cultured in ciPTEC medium containing phenol red free DMEM/F12 medium (Gibco/Invitrogen, Breda, The Netherlands) supplemented with 10% (v/v) fetal calf serum (FCS; MP Biomedicals, Uden, The Netherlands), insulin (5  $\mu\text{g}/\text{ml}$ ), transferrin (5  $\mu\text{g}/\text{ml}$ ), selenium (5 ng/ml), hydrocortisone (36 ng/ml), epithelial growth factor (10 ng/ml), and tri-iodothyronine (40 pg/ml) at  $33^{\circ}\text{C}$  in a

5% (v/v)  $\text{CO}_2$  atmosphere. Propagation of cells was maintained by subculturing the cells at a dilution of 1:3 to 1:6 at  $33^{\circ}\text{C}$ . For experiments, cells were cultured at  $33^{\circ}\text{C}$  to 40% confluency, followed by maturation for 7 days at  $37^{\circ}\text{C}$ . Experiments were performed on the cells between passages 30 and 40.

### 2.3. Quantitative PCR array

To study the gene expression of drug metabolism enzymes, ciPTEC were cultured and differentiated cells (7 days at  $37^{\circ}\text{C}$ ) were harvested. Total RNA was isolated using an RNeasy Mini kit (Qiagen, Venlo, The Netherlands) according to the manufacturer's recommendations. Subsequently, cDNA was generated using the Omniscript RT-kit (Qiagen) according to the manufacturer's recommendations. Following cDNA-synthesis, RT<sup>2</sup> Profiler PCR arrays (drug metabolism: phase I and phase II enzymes; Qiagen) were performed according to the manufacturer's recommendations, using a CFX96 Real-Time PCR detection system (Bio-rad, Veenendaal, The Netherlands). Quantification of gene expression was performed using the CFX96 system software (Bio-rad) and the web-based PCR array data analysis software (Qiagen). GAPDH was used as housekeeping gene, and relative expression levels were calculated as percentage as compared with GAPDH (100%).

### 2.4. Western blotting

To study the protein expression of UGT1A and UGT2B, ciPTEC were cultured and exposed to 0–2 mM of different uremic toxins for 48 h. After treatment, cells were harvested using RIPA buffer containing 1% (v/v) Igepal CA630, 0.5% (v/v) Nadeoxycholate, 0.1% (w/v) SDS, 0.01% (w/v) phenylmethane sulphonylfluoride, 3% (v/v) aprotinin and 1 mM Na-orthovanadate. Total protein (50  $\mu\text{g}$ ) was separated via SDS/PAGE using 10% (w/v) gels and blotted onto nitrocellulose membranes using the iBlot dry blotting system (Invitrogen). Afterwards, the membrane was blocked using Odyssey Blocking Buffer, (1:1 diluted with PBS; LI-COR Biosciences, Lincoln, NE, USA) during 1 h at RT. The membrane was then incubated overnight at  $4^{\circ}\text{C}$  with rabbit polyclonal UGT1A or UGT2B antibody (1:200; both Santa Cruz Biotechnology, Inc., Santa Cruz, CA, USA). Mouse monoclonal  $\beta$ -actin antibody (1:10,000; Sigma) was simultaneously incubated to serve as a protein loading control. Antibodies were diluted in Odyssey Blocking Buffer containing 0.1% (v/v) Tween-20. Afterwards, the membrane was thoroughly washed three times during 10 min with PBS containing 0.1% (v/v) Tween-20. The secondary antibodies, goat- $\alpha$ -mouse Alexa Fluor 680 (1:20,000; Invitrogen) and goat- $\alpha$ -rabbit IRDye 800 (1:20,000; Rockland, Gilbertsville, PA, USA), were incubated for 1 h at RT in Odyssey Blocking Buffer containing 0.1% (v/v) Tween-20 and 0.01% (w/v) SDS. The membrane was thoroughly washed, as described above, and then scanned using the Odyssey Infrared Imaging System (LI-COR Biotechnology). Intensity of the protein bands was quantified using the Odyssey Application software version 2.1.

### 2.5. Confocal microscopy

Cellular localization of UGT1A and UGT2B proteins was investigated using confocal microscopy. ciPTEC were seeded on 12-well Corning Costar Transwell Permeable Supports (type 3460, Corning Costar, NY, USA). Before seeding, the supports were coated with 50  $\mu\text{g}/\text{ml}$  collagen type IV for 2 h at  $37^{\circ}\text{C}$ . Subsequently, supports were washed with HBSS buffer (Gibco) and cells were seeded at a density of  $1.33 \times 10^5$  cells/cm<sup>2</sup>. Following maturation, as described above, cells were washed with wash solution (4% (v/v) FCS in HBSS) and fixed for 5 min with 2% (w/v) paraformaldehyde in HBSS. Next, cells were permeabilized for 10 min in HBSS with 0.3% (v/v) Triton and aspecific epitopes were blocked for 30 min with blocking buffer (2% (v/v) FCS, 0.5% (w/v) bovine serum albumin and 0.1% (v/v) Tween-20 in HBSS). Subsequently, the cells were incubated overnight at  $4^{\circ}\text{C}$  with rabbit polyclonal UGT1A or

UGT2B antibody (1:50 in blocking buffer, Santa Cruz Biotechnology) using dynamic conditions. Afterwards, cells were incubated for 30 min with the secondary antibody goat- $\alpha$ -rabbit Alexa568 (1:200, Molecular Probes, Invitrogen). Subsequently, ciPTEC were incubated for 1 h with a mouse monoclonal antibody against the tight junction protein ZO-1 (1:50 in blocking buffer, Invitrogen, CA, USA). Next, the cells were simultaneously incubated for 30 min with goat- $\alpha$ -mouse Alexa488 (1:200, Molecular Probes, Invitrogen) and DAPI nucleic acid stain (300 nm, Molecular Probes, Invitrogen). The slides were then mounted using Fluorescent Mounting Medium (DakoCytomation, Dako Netherlands b.v., Heverlee, Belgium). Between all incubation steps the cells were washed with wash solution. Fluorescence was examined using the Olympus FV1000 Confocal Laser Scanning Microscope (Olympus, UK) and images were captured using the Olympus software FV10-ASW version 1.7.

## 2.6. High-performance liquid chromatography (HPLC)

HPLC was used to measure UGT activity *via* the glucuronidation of 7-hydroxycoumarin (7-OCH), as described previously, [31] and *p*-cresol. To determine enzyme kinetics, ciPTEC were exposed to 7-OCH or *p*-cresol dissolved in HBSS at 37 °C and 4 °C (as negative control) using different concentrations (0–500  $\mu$ M) and different incubation times (0–5 h). When used,  $\beta$ -glucuronidase from *Helix pomatia* was added 1 h prior to incubation with 7-OCH (50  $\mu$ M for 3 h). In addition, UGT activity was also determined following exposure to uremic toxins for 48 h. Following treatment, ciPTEC were incubated with 10  $\mu$ M 7-OCH for 3 h at 37 °C. Before chromatography an aliquot of culture medium was collected and centrifuged at 12,000 $\times$ g for 3 min and 50  $\mu$ l of the supernatant was injected into the HPLC-system (Spectra-Physics Analytical, Spectrasystem SCM400). To measure 7-OCH and 7-OCH glucuronide (7-OCHG) the HPLC was equipped with a C18 HPLC column (GraceSmart RP 18 5u 150 $\times$ 4.6 mm; Grace, Breda, The Netherlands). Separation was performed at a flow rate of 1 ml/min with eluent A (95% (v/v) H<sub>2</sub>O, 5% (v/v) methanol and 0.2% (v/v) acetic acid) and eluent B (50% (v/v) H<sub>2</sub>O, 49% (v/v) acetonitrile and 1% (v/v) tetrahydrofuran) under the following gradient conditions: 0–3 min, 80–50% eluent A; 3–8 min, 50% eluent A; 8–9 min, 50–80% eluent A; 9–14 min, 80% eluent A. The compounds were detected at a wavelength of 316/382 nm. For the detection of *p*-cresyl sulfate and *p*-cresyl glucuronide, chromatography was performed on a C18 HPLC column (GraceSmart RP 18 5u 150 $\times$ 4.6 mm) with eluent A (95% (v/v) 50 mM KH<sub>2</sub>PO<sub>4</sub> (pH 3.0) and 5% (v/v) acetonitrile) and eluent B (50 mM KH<sub>2</sub>PO<sub>4</sub> (pH 3.0), methanol and acetonitrile in a 1:1:1 ratio) using the following gradient: 0–15 min, 100–20% eluent A; 15–16 min, 20–100% eluent A; 16–21 min, 100% eluent A. The flow rate was 1 ml/min and the *p*-cresol metabolites were detected at a wavelength of 220 nm. Standards of the compounds were also run in order to quantify the amount of metabolites found in the samples. Acquired data were processed with PC1000 software (Spectrasystem).

## 2.7. 3-[4,5-dimethylthiazol-2-yl]-2,5-diphenyl tetrazolium bromide (MTT) assay

Mitochondrial succinate dehydrogenase activity was assessed using the MTT assay. ciPTEC were cultured in a 96 well culture plate and exposed to 1 mM or 2 mM of uremic toxins for 48 h. Next, medium was removed and 20  $\mu$ l preheated (37 °C) MTT-solution (5 mg 3-[4,5-dimethylthiazol-2-yl]-2,5-diphenyl tetrazolium bromide/ml ciPTEC medium) was added and incubated for 4 h at 37 °C. Afterwards, MTT-solution was removed, followed by the addition of 200  $\mu$ l DMSO to dissolve produced formazan crystals. The extinction of the solution was measured at 570 nm using a Benchmark Plus Microplate Spectrophotometer (Bio-rad).

## 2.8. Flow cytometry

In this study, flow cytometry was used to study ciPTEC morphology and viability. Cells were cultured in 12-well culture plates and treated for 48 h with 2 mM of uremic toxins. After incubation, cells were harvested using trypsin-EDTA and centrifuged at 600 $\times$ g during 5 min. Subsequently, supernatant was removed and the cell pellet was resuspended in 100  $\mu$ l PBS containing 4% (w/v) paraformaldehyde and 0.1% (v/v) saponin followed by 10 min incubation on ice. Subsequently, samples were centrifuged (600 $\times$ g for 5 min) and resuspended in 100  $\mu$ l PBS. Samples were acquired on a BD FACSCalibur (Becton Dickinson, Breda, The Netherlands). Analysis was performed using Flow Jo software (TreeStar, Ashland, USA), gating on live cells.

## 2.9. High-resolution respirometry

Cells were cultured in T25 culture flasks and treated for 48 h with 2 mM indole-3-acetic acid. Subsequently, cells were harvested using trypsin-EDTA and centrifuged at 1500 $\times$ g during 5 min. Afterwards, the supernatant was removed and the cell pellet was resuspended in ciPTEC medium to obtain a suspension of approximately  $1 \times 10^6$  cells/ml. Two milliliters of the cell suspension was used to measure cellular oxygen consumption. Oxygen consumption was measured at 37 °C using polarographic oxygen sensors in a two-chamber Oxygraph (Oroboros Instruments, Innsbruck, Austria) using an established protocol [32]. The cells were allowed to respire at basal level for at least 10 min until the flux was stable, representing routine respiration (R). Next, leak respiration (L) was determined by addition of the specific mitochondrial ATP synthase inhibitor oligomycin A (omy; 2.5  $\mu$ M). Then, maximal ETS capacity (E) was quantified using increasing concentrations of the mitochondrial uncoupler *p*-trifluoromethoxy carbonyl cyanide phenyl hydrazone (FCCP; 2.5  $\mu$ M maximal concentration). Finally, non-mitochondrial respiration (ROX) was assessed by adding a maximal (0.5  $\mu$ M) concentration of the specific mitochondrial complex I inhibitor rotenone (ROT) followed by the Complex III inhibitor antimycin A (AA; 2.5  $\mu$ M).

## 2.10. Kinetic analysis and statistics

Statistics were performed using GraphPad Prism 5.02 *via* one-way analysis of variance (ANOVA) followed by Dunnett's Multiple Comparison Test or an unpaired *t* test. Differences between groups were considered to be statistically significant when *p* < 0.05. The software was also used to perform linear and nonlinear regression analysis (Michaelis–Menten) and correlation analysis (Spearman).

## 3. Results

### 3.1. Selection of uremic toxins

In our study, 13 uremic solutes were selected containing one water-soluble solute (oxalate, Ox) and 12 protein-bound solutes. The latter group contained 4 tryptophan metabolites (indoxyl sulfate, IS; indole-3-acetic acid, I3A; kynurenic acid, KA; and quinolinic acid, QA), six phenols (phenylacetic acid, PHA; phenyl glucuronide, PHG; phenyl sulfate, PHS; *p*-cresol, pC; *p*-cresyl sulfate, pCS; and *p*-cresyl glucuronide, pCG), one hippurate (hippuric acid, HA) and one polyamine (putrescine, Pu). Moreover, a mix of several uremic toxins (Mix) was used, consisting of putrescine, oxalate, indoxyl sulfate and *p*-toluenesulfonic acid, a previously described phenolic model compound (1:1:1:1) [33]. This specific mix was chosen because it contained different classes of solutes, of which the stock solutions were all prepared in the same solvent (e.g. milli-Q).

### 3.2. Expression and activity of UGT in ciPTEC

Extrahepatic glucuronidation occurs mainly in the kidney and UGT expression and activity were demonstrated in both human and rat primary proximal tubule cells [8,34,35]. We used a recently established human renal proximal tubule cell line, [30,36] in which phase I and phase II drug metabolism enzyme expression levels were studied, with an emphasis on the class of UGT enzymes. A complete overview of the drug metabolism enzyme expression in ciPTEC is provided in Fig. S1. This figure clearly demonstrates that ciPTEC express a broad range of drug metabolism enzymes, including cytochrome p450 (CYP), sulfotransferase (SULT) and glutathione S-transferase (GST) enzymes, next to members of the UGT family. Fig. 1A shows that the gene expression of 18 UGTs was detected in ciPTEC of which UGT1A1, 1A9, 2B7, 2B10 and 2B28 were most abundantly expressed compared with GAPDH, with a relative expression of 11%, 2143%, 16%, 145% and 9%,

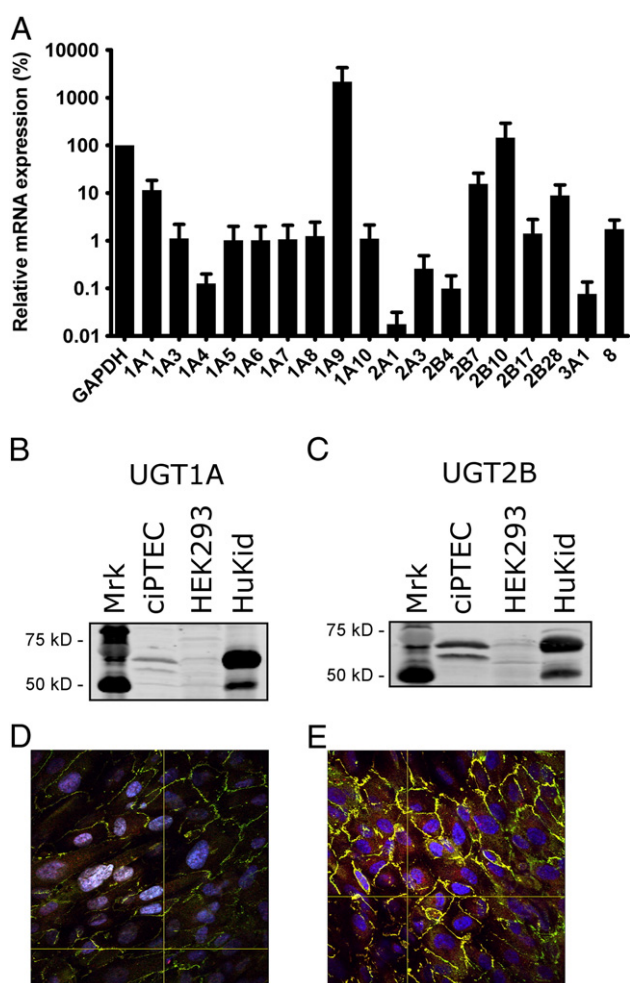


**Fig. 1.** Expression of UGTs in ciPTEC. (A) Differentiated ciPTEC were harvested and total mRNA was isolated. Afterwards, cDNA was synthesized and UGT gene expression was studied using a qPCR array. Relative expression was calculated using the household gene GAPDH (100%). Bars represent mean  $\pm$  SEM of two experiments. (B–C) UGT1A and UGT2B protein expression was studied by Western blotting. Proteins were separated via SDS/PAGE and blotted onto nitrocellulose membranes. Lysates of HEK293 cells were used as a negative control and homogenates from human kidney (HuKid) were used as positive control. Both UGT1A and UGT2B were detected at 68 kD. (D–E) Confocal microscopy was used to study intracellular localization of UGTs in ciPTEC. Following maturation, cells were fixed and permeabilized and subsequently stained using an antibody against UGT1A or UGT2B and ZO-1. Detection was performed using Alexa568 for UGTs (red) and Alexa488 for ZO-1 (green) labeled secondary antibodies. Nucleus was stained with DAPI (blue). (B–E) Representative images of two independent experiments.

respectively. Furthermore, using Western blotting UGT1A and 2B family members were detected in ciPTEC, with the predicted molecular weight of the enzymes (approximately 68 kD; Fig. 1B–C). Protein expression of the enzymes was also demonstrated in human kidney lysates, whereas their expression was absent in human embryonic kidney (HEK293) cells. Glucuronide formation occurs in the cytosol, and confocal microscopy demonstrated that both UGT1A and 2B enzymes exhibit cytosolic localization in ciPTEC (Fig. 1D–E). Moreover, expression of tight junction protein 1 (ZO-1) revealed that ciPTEC form tight junctions and that the cells maintain their epithelial characteristics during culturing.

To determine whether the UGTs were enzymatically active, a glucuronidation assay was performed using 7-OHC as a substrate. A concentration-dependent formation of 7-OHC glucuronide was observed (Fig. 2A), and curve fitting revealed an apparent  $K_m$  of  $12 \pm 2 \mu\text{M}$  and a  $V_{max}$  of  $76 \pm 3 \text{ pmol/min/mg}$ . Glucuronidation was demonstrated to be linear up to 5 h (Fig. 2B). Furthermore, as depicted in Fig. 2A and 2B, 7-OHC metabolism was completely absent at  $4^\circ\text{C}$ , indicating enzyme-dependent conjugation. Glucuronidation of  $50 \mu\text{M}$  7-OHC was concentration-dependently inhibited by  $\beta$ -glucuronidase with an approximate  $IC_{50}$  value of 50 U/ml, as demonstrated in Fig. 2C.

### 3.3. Uremic toxins decrease UGT activity

Next, it was investigated whether exposure of ciPTEC to uremic toxins could influence 7-OHC glucuronidation Fig. 3 shows that a myriad of uremic toxins belonging to three different physico-chemical classes, viz. tryptophan metabolites, phenols and water-soluble compounds, concentration-dependently inhibited the glucuronidation of 7-OHC. Kynurenic acid, indole-3-acetic acid, phenylacetic acid and a mixture of uremic toxins most potently inhibited UGT activity (Fig. 3A–C). At the highest concentration, these toxins decreased glucuronide formation by 52%, 44%, 36% and 50%, respectively. In addition, at the same concentration, indoxyl sulfate, phenyl sulfate, oxalate, putrescine and hippuric acid inhibited the formation of 7-OHCG by 32%, 30%, 16%, 18% and 32%, respectively. In contrast, quinolinic acid and phenyl glucuronide did not affect 7-OHC metabolism.

A decline in enzyme activity is often secondary to a decrease in protein expression, therefore, the impact of uremic toxins on UGT expression was examined. Exposure of ciPTEC to none of the different toxins reduced UGT1A and UGT2B protein expression with more than 15%, with both tested concentrations, compared to control. A representative sample of toxins is shown in Fig. 4, and the other toxins in Fig. S2.

### 3.4. P-cresol metabolism and impact on glucuronidation

To further investigate the mode of inhibition, ciPTEC were exposed to p-cresol, which can be metabolized to both p-cresyl sulfate and p-cresyl glucuronide [37]. Fig. 5A shows that p-cresol is indeed conjugated to glucuronic acid in ciPTEC and a concentration-dependent formation of p-cresyl glucuronide is demonstrated with a calculated  $K_m$  of  $33 \pm 13 \mu\text{M}$  and a  $V_{max}$  of  $266 \pm 25 \text{ pmol/min/mg}$ . In contrast, ciPTEC did not metabolize p-cresol to p-cresyl sulfate (data not shown), despite the expression of multiple sulfotransferases, the enzymes that catalyze sulfation reactions (Fig. S1). Furthermore, HPLC revealed that p-cresol inhibited 7-OHCG formation by 72% (Fig. 5B). Yet, both p-cresol metabolites also inhibited UGT activity with approximately 20%.

### 3.5. Uremic toxins inhibit mitochondrial metabolism

Reduction of MTT is mainly dependent on mitochondrial succinate dehydrogenase activity [38]. Our results indicate that the majority of the toxins tested (e.g. putrescine, oxalate, indoxyl sulfate) did not significantly decrease MTT reduction with more than 15% compared to control (Fig. S3). Yet, p-cresol, p-cresyl sulfate and p-cresyl glucuronide significantly reduced mitochondrial succinate dehydrogenase

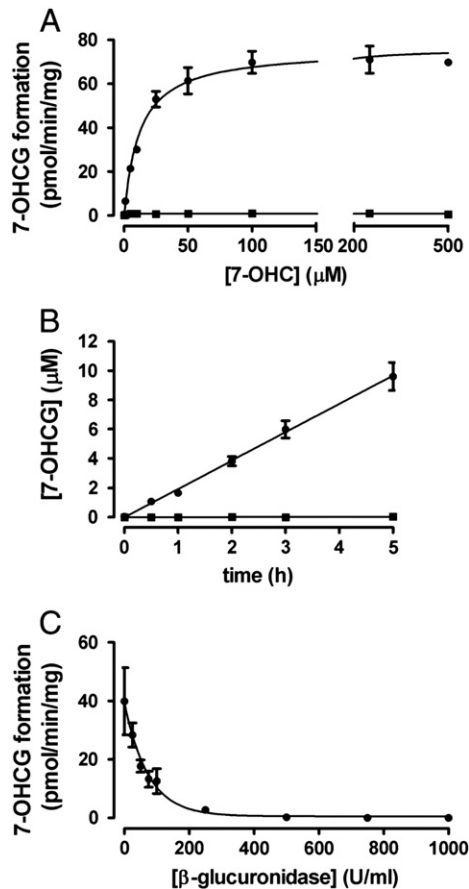


**Fig. 2.** UGTs are functionally active. HPLC was used to study UGT activity via 7-OHC glucuronidation. Cells were incubated with 7-OHC (0–500 μM) for 0–5 h at 37 °C (●) or 4 °C (negative control; ■). To further demonstrate specificity of the HPLC method, cells were incubated with 50 μM 7-OHC for 3 h in the presence of β-glucuronidase (0–1000 u/ml). (A) Concentration-dependent formation of 7-OHCG. (B) Time curve of 7-OHC glucuronidation. (C) β-glucuronidase inhibits glucuronide formation. Standards of 7-OHCG were also analyzed in order to quantify the amount of glucuronide found in the samples. Acquired HPLC data were processed with PC1000 software (Spectrasystem). Nonlinear and linear regression analyses were performed using Graphpad Prism 5.02. Results are presented as mean ± SEM of three independent experiments performed in triplicate.

activity with 28%, 21% and 14%, respectively (Fig. 6A). In addition, the toxins that most potently inhibited UGT activity (*i.e.* indole-3-acetic acid, phenylacetic acid and a mixture of uremic toxins) also significantly decreased MTT reduction at the highest concentration by 28%, 26% and 33%, respectively. Moreover, we observed a significant correlation between the two parameters studied, with a calculated Spearman  $r$  of 0.69 ( $p < 0.005$ ; Fig. 6B). Since the MTT assay is often used to study cell viability, we aimed to confirm that the observed correlation was not due to the induction of cell death by uremic toxins. Flow cytometry revealed that exposure of ciPTEC to the solutes that had the most pronounced impact on cellular and mitochondrial metabolism did not affect cell morphology nor the percentage of living cells as compared with untreated cells (Fig. S4).

### 3.6. Inhibition of mitochondrial respiration by indole-3-acetic acid

Mitochondrial succinate dehydrogenase plays an essential role in the electron transfer chain and the tricarboxylic acid cycle (*i.e.* citric acid cycle) [39]. Therefore, we investigated the impact of indole-3-acetic acid on the OXPHOS system, since this solute had the most profound effect on both 7-OHC glucuronidation and MTT reduction. High-resolution

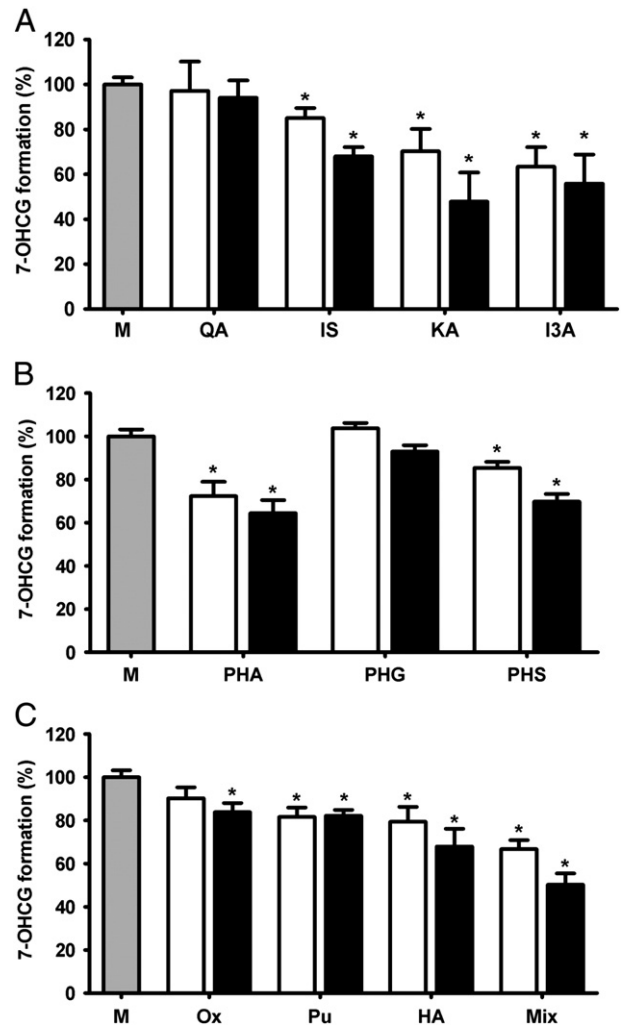


**Fig. 3.** Uremic toxins inhibit 7-OHC glucuronidation. Impact of uremic toxin exposure on 7-OHC glucuronidation was studied using HPLC. Cells were exposed for 48 h to ciPTEC medium (gray bar), 1 mM (white bars) or 2 mM (black bars) of several uremic toxins belonging to three different physico-chemical classes: (A) tryptophan metabolites, (B) phenols and (C) water-soluble compounds. Following treatment, ciPTEC were incubated for 3 h with 10 μM 7-OHC. Afterwards, an aliquot of culture medium was collected and injected into the HPLC-system. Standards of 7-OHCG were also analyzed in order to quantify the amount of glucuronide found in the samples. Acquired HPLC data were processed with PC1000 software (Spectrasystem). Statistical analysis was performed via one-way ANOVA followed by Dunnett's Multiple Comparison Test for each toxin. Results are presented as mean ± SEM of three experiments performed in duplicate or triplicate. \* =  $p < 0.05$  compared with control. HA, hippuric acid; I3A, indole-3-acetic acid; IS, indoxyl sulfate; KA, kynurenic acid; M, medium; Mix, uremic toxin mix; Ox, oxalate; PHG, phenyl glucuronide; PHS, phenyl sulfate; PHA, phenylacetic acid; Pu, putrescine; QA, quinolinic acid.

respirometry revealed that basal mitochondrial respiration (R; ROUTINE), electron transport that was not coupled to ATP production (L; LEAK) and non-mitochondrial respiration (ROX; residual oxygen consumption) was not compromised by indole-3-acetic acid (Fig. 7A–B), further supporting the impression that uremic toxins did not induce cell death in ciPTEC. In contrast, the maximum capacity of the electron transport system (E; ETS) was reduced from  $221 \pm 21$  pmol/s ·  $10^6$  cells in untreated cells to  $182 \pm 17$  pmol/s ·  $10^6$  cells in ciPTEC exposed to indole-3-acetic acid, indicating that treatment caused a reduction in the reserve capacity for energy production. Fig. 7C shows that exposure of the cells to indole-3-acetic acid resulted in a significantly increased netRoutine/ETS ratio, with a 1.3 fold change. This signifies that a higher proportion of the maximum capacity of the OXPHOS system is activated to drive ATP synthesis, and implies that ciPTEC exposed to uremic toxins have a limited ability to supply energy for other cellular processes, such as enzymatic activity.

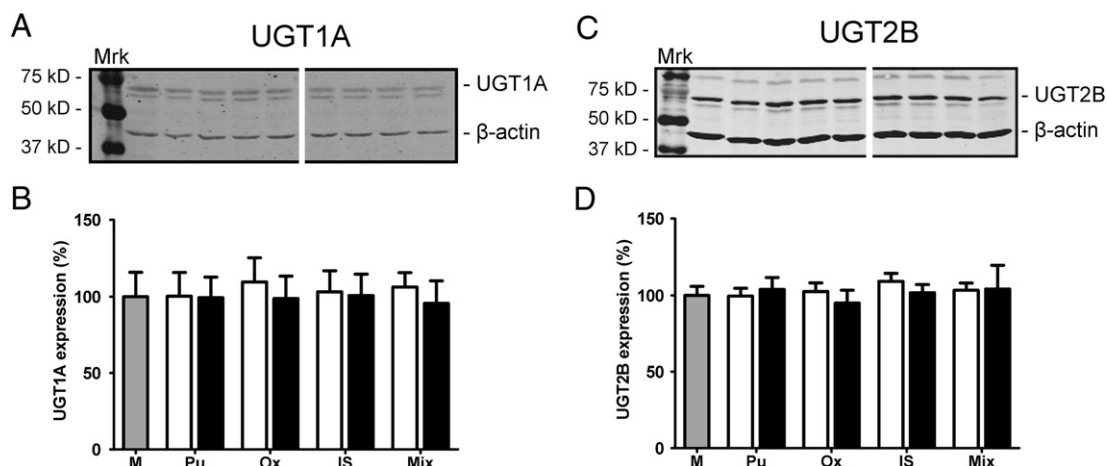


**Fig. 4.** UGT1A and UGT2B protein expression is not affected by uremic toxins. UGT1A and UGT2B protein expression was studied *via* Western blot. Cells were exposed for 48 h to ciPTEC medium (gray bar), 1 mM (white bars) or 2 mM (black bars) of several uremic toxins. (A/C) Afterwards cells were lysed and proteins were separated *via* SDS/PAGE and blotted onto nitrocellulose membranes. Both UGT1A and UGT2B were detected at 68 kD. (B/D) Fluorescence of the specific protein bands was determined using the Odyssey Infrared Imaging System. Bars represent mean  $\pm$  SEM of the UGT band intensities corrected for  $\beta$ -actin from 3 independent experiments. IS, indoxyl sulfate; M, medium; Mix, uremic toxin mix; Ox, oxalate; Pu, putrescine.

#### 4. Discussion

This study reports for the first time that multiple uremic toxins directly inhibit the function of an important class of phase II drug metabolism enzymes, namely UGTs, in human renal proximal tubule cells. Our results showed that uremic toxin-induced UGT inhibition was independent of an effect on protein expression, and inhibition seemed to

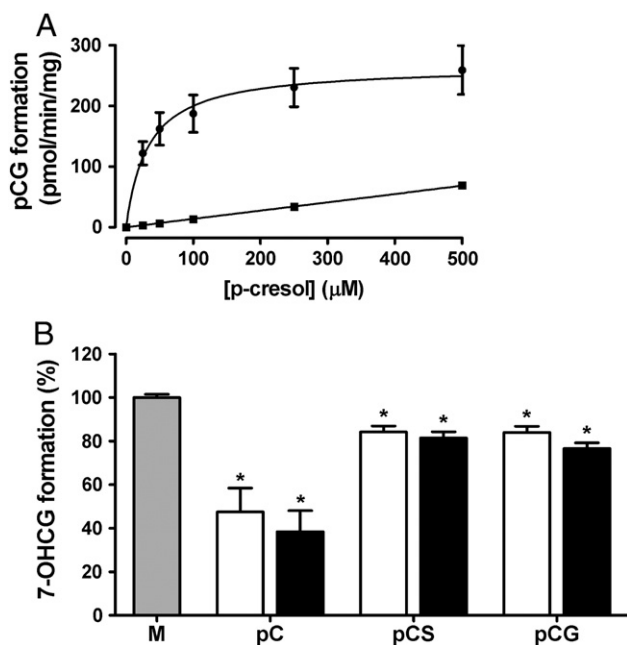


**Fig. 5.** P-cresol glucuronidation and impact on UGT activity by cresols. (A) HPLC was used to study p-cresol glucuronidation. Cells were incubated with p-cresol (0–500  $\mu$ M) for 1 h at 37  $^{\circ}$ C ( $\bullet$ ) or 4  $^{\circ}$ C (negative control;  $\blacksquare$ ). (B) Cells were exposed for 48 h to ciPTEC medium (gray bar), 1 mM (white bars) or 2 mM (black bars) of p-cresol or the metabolites. Following treatment, ciPTEC were incubated for 3 h with 10  $\mu$ M 7-OHC. After incubation with p-cresol or 7-OHC, an aliquot of culture medium was collected and injected into the HPLC-system. Standards of the compounds were also analyzed in order to quantify the amount of metabolites found in the samples. Acquired HPLC data were processed with PC1000 software (Spectrasystem). Nonlinear analysis was performed using Graphpad Prism 5.02 and statistical analysis was performed *via* one-way ANOVA followed by Dunnett's Multiple Comparison Test for each toxin. Results are presented as mean  $\pm$  SEM of three independent experiments performed in duplicate or triplicate. \* =  $p < 0.05$  compared with control. M, medium; pC, p-cresol; pCG, p-cresyl glucuronide; pCS, p-cresyl sulfate.

occur in both a competitive (e.g. p-cresol) and non-competitive fashion (e.g. p-cresyl sulfate). It is likely that most uremic solutes act as non-competitive inhibitors of UGT activity, since the majority of these compounds are end-products of endogenous metabolism.

To further unravel the mode of inhibition, mitochondrial respiration was studied and the results indicated that indole-3-acetic acid reduced the reserve capacity of the electron transport system. This finding provides more insight into the mechanism by which uremic toxins possibly inhibit UGT activity. As stated before, glucuronide formation is dependent on the availability of UDPGA, the donor of the glucuronide moiety [23]. UDPGA is formed from UDP-glucose by UDP-glucose dehydrogenase using nicotinamide adenine dinucleotide ( $\text{NAD}^+$ ), a coenzyme that plays an important role in energy metabolism [40]. In the mitochondria, enzymes of the citric acid cycle reduce  $\text{NAD}^+$  to NADH. Subsequently, NADH is oxidized by complex I of the electron transport chain during OXPHOS-mediated ATP production, resulting in the conversion of NADH to  $\text{NAD}^+$  [40]. Therefore, we postulate that a reduction in the activity of the mitochondrial electron transport chain induced by uremic toxins, as demonstrated in this study, caused a drop in  $\text{NAD}^+$  levels and, consequently, led to depletion of UDPGA, thereby decreasing UGT-mediated metabolism.

*De novo* synthesis of  $\text{NAD}^+$  in mammals is dependent on tryptophan metabolism *via* the kynurenine pathway [40]. Dietary tryptophan is converted to kynurenine by tryptophan 2,3-dioxygenase and indoleamine 2,3-dioxygenase, which are both considered the rate-limiting steps in this pathway [40,41]. Kynurenine can, subsequently, be metabolized to kynurenic acid by kynurenine aminotransferase or, *via* several other enzymatic steps, to quinolinic acid [41]. The latter metabolite is used by quinolinic acid phosphoribosyl transferase to form  $\text{NAD}^+$ . Interestingly, it is known that plasma tryptophan levels are significantly diminished in CKD patients [42]. Furthermore, Fukuwatari et al. reported that  $\text{NAD}$  ( $\text{NAD}^+ + \text{NADH}$ ) concentrations were decreased in the liver, kidney and blood of rats with adenine-induced renal failure [43]. Thus, it is likely that UDPGA levels are reduced in patients with CKD due to altered tryptophan metabolism, resulting in a reduced UGT activity.

To our knowledge, this is the first report to demonstrate the influence of uremic toxins on mitochondrial metabolism and respiration in human proximal tubule cells. Previously, Owada et al. demonstrated that indoxyl sulfate stimulated renal mitochondrial superoxide production in rats [44]. Dzurik et al. described that hippuric acid reduced ammonia production by P-dependent mitochondrial glutamine in kidney homogenates of acidified rats [45]. Furthermore, using isolated rat liver mitochondria, Kitagawa revealed that p-cresol

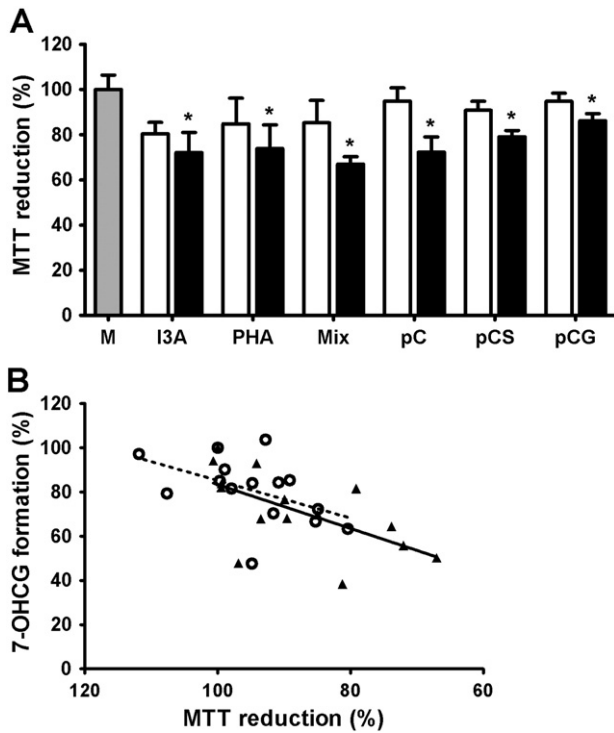


**Fig. 6.** Inhibitory effect of uremic toxins on MTT reduction. (A) The MTT assay was used to study the impact of uremic toxins on mitochondrial metabolism. Cells were exposed for 48 h to ciPTEC medium (gray bar), 1 mM (white bars) or 2 mM (black bars) of several uremic toxins. Afterwards, cells were incubated for 4 h with MTT-medium at 37 °C. Subsequently, produced formazan crystals were dissolved in DMSO and extinction was measured at 570 nm. Statistical analysis was performed via one-way ANOVA followed by Dunnett's Multiple Comparison Test for each toxin. Results are presented as mean  $\pm$  SEM of three independent experiments performed in triplicate. \* =  $p < 0.05$  compared with control. I3A, indole-3-acetic acid; M, medium; Mix, uremic toxin mix; pC, p-cresol; pCG, p-cresyl glucuronide; pCS, p-cresyl sulfate; PHA, phenylacetic acid. (B) Correlation between UGT activity and MTT reduction. Cells were exposed for 48 h to 1 mM (○) or 2 mM (▲) of several uremic toxins and 7-OHCG glucuronidation and MTT reduction were investigated. Nonparametric Spearman correlation analysis revealed a significant association between the reduction in glucuronidation and mitochondrial dehydrogenase activity when ciPTEC were treated with 2 mM of uremic toxins ( $r = 0.69$ ;  $p < 0.005$ ). Following exposure to 1 mM of uremic toxins, no significant correlation was observed ( $r = 0.48$ ;  $p = 0.07$ ).

inhibited state 3 respiration without affecting oxidative phosphorylation [46]. Yet, p-cresol is no longer regarded as a uremic toxin, [37] and it remains to be elucidated whether its major metabolite, p-cresyl sulfate, has a similar impact on mitochondrial respiration. Additionally, Riegel et al. reported that treatment of hepatocytes with ultrafiltrates of patients treated with high-flux membrane dialyzer significantly diminished MTT reduction [47]. However, the effect correlated with an increased LDH release, a marker of cell injury, and the decrease in metabolic activity might have been due to hepatotoxicity. These findings, together with our current results, suggest that uremic toxins might directly influence mitochondrial activity in different organs.

The uremic toxin concentrations used in this study do not always reflect the plasma levels determined in CKD patients, for instance the highest concentration reported for kynurenic acid is 50  $\mu$ M, whereas the maximal uremic concentration for hippuric acid and phenylacetic acid are 2.6 and 7.7 mM, respectively [48,49]. An overview of the maximal uremic concentrations of the solutes used in the present study are provided in Table S1, and for a detailed description of uremic toxin concentrations the interested reader is referred to reviews by the European Uremic Toxin Work Group [48,50].

Since UGTs are located in the cytosol, enzyme activity depends on the intracellular levels of substrates rather than substrate concentrations in the blood. Uptake of uremic toxins in renal proximal tubules is fairly well characterized and shown to be dependent on a wide

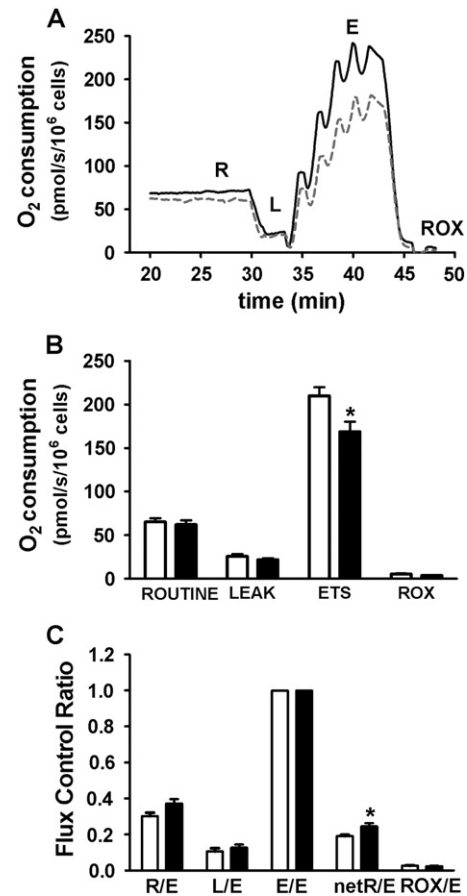


**Fig. 7.** Reduction in mitochondrial respiration by indole-3-acetic acid. High-resolution respirometry was used to measure mitochondrial oxygen consumption. Cells were treated for 48 h with ciPTEC medium (white bar) or 2 mM indole-3-acetic acid (black bar) and oxygen consumption was measured at 37 °C using polarographic oxygen sensors in an Oxygraph. (A) Online high-resolution respirometry traces of mitochondrial respiration in a representative experiment with control (solid line) and indole-3-acetic acid (dashed line) treated cells. Titrations: ROUTINE (R) respiration (intact cells), omy (LEAK respiration; L), FCCP (ETS capacity; E), Rot and AA (ROX). (B) Quantification of cellular respiration. (C) Quantification of cellular respiration corrected for electron transport system capacity. Statistical analysis was performed via an unpaired *t* test. Results are presented as mean  $\pm$  SEM of three experiments performed in duplicate. \* =  $p < 0.05$  compared with control.

variety of transport proteins. Both organic anion transporter (OAT) 1 and OAT3, as well as organic anion transporting polypeptide 4C1, play an important role in the tubular uptake of uremic toxins [51–54]. In addition, it has been demonstrated that the multi-ligand receptor megalin is involved in the endocytotic uptake of a specific group of uremic toxins, i.e. advanced glycation end products [55]. Previously, Masereeuw et al. demonstrated that methyl hippuric acids accumulate in the isolated perfused rat kidney during secretory transport [56,57]. They reported that 2-methyl hippuric acid levels were 175-times higher in renal tissue compared to the perfusate and 4-methyl hippuric acid concentrations were even 600-times higher. Thus, it is likely that intracellular uremic toxin concentrations are much higher than total plasma concentrations. Therefore, it is complicated to extrapolate our findings to the clinical situation.

The present study demonstrates that UGT1A1, 1A9, 2B7 and 2B28 are highly expressed in ciPTEC, which corroborates previous reports on proximal tubule cells [21,34]. Lash et al. described that primary human proximal tubule cells (PTEC) express UGT1A1, 1A6 and 2B7 on protein level [34]. Furthermore, they postulated that UGT2B7 is the major UGT isoform present in PTEC cells. In the study from Ohno and coworkers, gene expression was demonstrated for UGT1A5, 1A6, 1A7, 1A9, 2B4, 2B7 and 2B17 in human kidney tissue, and they reported that UGT1A9 and 2B7 were most abundantly expressed [21]. Next to

members of the UGT family, ciPTEC were currently demonstrated to have RNA expression of phase I enzymes, such as CYP3A4, CYP4A11, CYP2D6, that have previously been detected in primary PTEC by Lash et al. [34]. Additionally, the phase II enzymes GSTA4, GSTP, GSTT and SULT1A3 were demonstrated in our current study, as well as in primary PTEC. Taken together, ciPTEC have a similar phase I and phase II enzyme expression profile compared with primary PTEC, indicating that this cell line is a suitable model to study extrahepatic drug metabolism. Together with the endogenous expression of renal influx and efflux drug transporters, previously described by our group, [30] these data demonstrate that human ciPTEC is a unique tool to study renal pharmacokinetics.

The majority of studies investigating the effect of renal failure on drug metabolism focused on CYP enzymes. For instance, Leblond et al. demonstrated that during CKD, both hepatic protein and gene expression of CYP2C11, CYP3A1 and CYP3A2 decreased in rats, which correlated with a decreased metabolism of aminopyrine and erythromycin [58,59]. The same group also showed that 48 h exposure of HK-2 cells to serum from uremic rats decreased the protein expression of CYP3A1, suggesting a role for uremic toxins in this process [60]. Moreover, using rat liver microsomes, Sun et al. described that indoxyl sulfate and 3-carboxy-4-methyl-5-propyl-2-furanpropanoic acid (CMPF) directly inhibited CYP3A-mediated metabolism of erythromycin [61]. With regard to phase II drug metabolism, Simard et al. demonstrated that N-acetyltransferase (NAT)1 and NAT2 expression decreased in the liver of CRF rats accompanied by a decrease in NAT2-mediated N-acetylation of p-aminobenzoic acid [9]. Furthermore, expression of both NAT1 and NAT2 decreased in rat hepatocytes following exposure to uremic serum, possibly via the action of parathyroid hormone, a known uremic toxin [9]. Taken together, there is a clear impact of uremic solutes on both phase I and phase II drug metabolism.

Hepatic and renal transporters play an important role in xenobiotic handling. Previously, our group described that several uremic toxins, including hippuric acid and indoxyl sulfate, inhibited transport by two important renal efflux transporters, namely breast cancer resistance protein and multidrug resistance protein 4 [33]. Huang et al. showed that uremic plasma, obtained from rats with CRF, inhibited p-glycoprotein-mediated transport [62]. Moreover, it is demonstrated that CMPF and hippuric acid inhibited the uptake by the renal uptake transporter OAT3 [51]. The impact of uremic toxins on the functionality of multiple transporters in those reports, and the inhibition of enzyme activity described in this study, indicate that the altered drug disposition observed in CKD patients can be attributed, at least in part, to uremic retention solutes.

In the present study, renal glucuronidation was solely studied *in vitro* using the ciPTEC model, which could differ from *in vivo* metabolism. Generally, UGT activity is studied using microsomes isolated from the organ of interest; however, by using a complete cell model instead of microsomes, we were able to unravel the possible mechanism via which uremic toxins indirectly influence UGT functionality. Moreover, it is known that there are species differences in renal glucuronidation [63], which did not hamper our study since ciPTEC are of human origin. Another possible drawback of the present study is that we studied renal metabolism, while during CKD, xenobiotics are metabolized mainly in the liver and intestine. However, it is known that both renal and non-renal clearance are affected in CKD patients [14], therefore we postulate that our results uncovered a general mechanism via which uremic toxins can diminish both renal and non-renal UGT activity, irrespective of the tissue-specific UGT expression profiles [21].

A main feature of CKD is the dysfunction of multiple organs and alterations in xenobiotic elimination pathways, however, the pathophysiological mechanism underlying these changes are not fully elucidated. In this study we demonstrated that a wide variety of uremic toxins, belonging to several physico-chemical classes, inhibited renal glucuronidation, most likely by reducing the reserve capacity of the energy-generating OXPHOS system. Our results provide additional insight into the widespread toxic effect of uremic solutes and depict a novel pathway via which uremic toxins impede renal metabolic

function and may have a clinically significant impact on drug disposition in patients with CKD.

Supplementary data to this article can be found online at <http://dx.doi.org/10.1016/j.bbadis.2012.09.006>.

## Disclosures

None.

## Acknowledgements

This work was funded by the Dutch Kidney Foundation (grant number IK08.03). M.J.G. Wilmer was supported by a grant from the Dutch government to the Netherlands Institute for Regenerative Medicine (NIRM, grant no. FES0908) and J. Jansen received funding from the Bio-Medical Materials Institute (Project P3.01 BioKid), co-funded by the Dutch Ministry of Economic Affairs, Agriculture and Innovation. J.G. Hoenderop was supported by an EURYI award from the European Science Foundation. The authors would like to thank A. Bilos for excellent technical support regarding the HPLC measurements. In addition, we thank A.E.M. Seegers for assisting in the experimental work.

## References

- [1] A.W. Dreisbach, J.J. Lertora, The effect of chronic renal failure on drug metabolism and transport, *Expert Opin. Drug Metabol. Toxicol.* 4 (2008) 1065–1074.
- [2] H. Sun, L. Frassetto, L.Z. Benet, Effects of renal failure on drug transport and metabolism, *Pharmacol. Ther.* 109 (2006) 1–11.
- [3] R.K. Verbeeck, F.T. Musuamba, Pharmacokinetics and dosage adjustment in patients with renal dysfunction, *Eur. J. Clin. Pharmacol.* 65 (2009) 757–773.
- [4] A. Yavuz, C. Tetta, F.F. Ersoy, V. D'intini, R. Ratanarat, C.M. De, M. Bonello, V. Bordini, G. Salvatori, E. Andrikos, G. Yakupoglu, N.W. Levin, C. Ronco, Uremic toxins: a new focus on an old subject, *Semin. Dial.* 18 (2005) 203–211.
- [5] N. Jourde-Chiche, L. Dou, C. Cerini, F. Gnat-George, R. Vanholder, P. Brunet, Protein-bound toxins—update 2009, *Semin. Dial.* 22 (2009) 334–339.
- [6] R. Vanholder, L.S. Van, G. Glorieux, What is new in uremic toxicity? *Pediatr. Nephrol.* 23 (2008) 1211–1221.
- [7] T.W. Meyer, The removal of protein-bound solutes by dialysis, *J. Ren. Nutr.* 22 (2012) 203–206.
- [8] J.W. Lohr, G.R. Willsky, M.A. Acara, Renal drug metabolism, *Pharmacol. Rev.* 50 (1998) 107–141.
- [9] E. Simard, J. Naud, J. Michaud, F.A. Leblond, A. Bonnardeaux, C. Guillemette, E. Sim, V. Pichette, Downregulation of hepatic acetylation of drugs in chronic renal failure, *J. Am. Soc. Nephrol.* 19 (2008) 1352–1359.
- [10] D.N. Bateman, R. Gokal, T.R. Dodd, P.G. Blain, The pharmacokinetics of single doses of metoclopramide in renal failure, *Eur. J. Clin. Pharmacol.* 19 (1981) 437–441.
- [11] R.K. Verbeeck, Glucuronidation and disposition of drug glucuronides in patients with renal failure. A review, *Drug Metab. Dispos.* 10 (1982) 87–89.
- [12] M.B. Howie, E. Bourke, Metabolism of p-aminobenzoic acid in the perfused livers of chronically uremic rats, *Clin. Sci. (Lond.)* 56 (1979) 9–14.
- [13] R. Osborne, S. Joel, K. Grebenik, D. Trew, M. Slevin, The pharmacokinetics of morphine and morphine glucuronides in kidney failure, *Clin. Pharmacol. Ther.* 54 (1993) 158–167.
- [14] A.W. Dreisbach, The influence of chronic renal failure on drug metabolism and transport, *Clin. Pharmacol. Ther.* 86 (2009) 553–556.
- [15] Y.G. Kim, J.G. Shin, S.G. Shin, I.J. Jang, S. Kim, J.S. Lee, J.S. Han, Y.N. Cha, Decreased acetylation of isoniazid in chronic renal failure, *Clin. Pharmacol. Ther.* 54 (1993) 612–620.
- [16] V. Uchaipichat, P.I. Mackenzie, X.H. Guo, D. Gardner-Stephen, A. Galetin, J.B. Houston, J.O. Miners, Human UDP-glucuronosyltransferases: isoform selectivity and kinetics of 4-methylumbelliferone and 1-naphthol glucuronidation, effects of organic solvents, and inhibition by diclofenac and probenecid, *Drug Metab. Dispos.* 32 (2004) 413–423.
- [17] J. Zhou, T.S. Tracy, R.P. Remmel, Correlation between bilirubin glucuronidation and estradiol-3-glucuronidation in the presence of model UDP-glucuronosyltransferase 1A1 substrates/inhibitors, *Drug Metab. Dispos.* 39 (2011) 322–329.
- [18] N. Meert, E. Schepers, G. Glorieux, L.M. Van, J.L. Goeman, M.A. Waterloos, A. Dhondt, E.J. Van der, R. Vanholder, Novel method for simultaneous determination of p-cresylsulphate and p-cresylglucuronide: clinical data and pathophysiological implications, *Nephrol. Dial. Transplant.* 27 (2012) 2388–2396.
- [19] T. Niwa, T. Miyazaki, S. Tsukushi, K. Maeda, Y. Tsubakihara, A. Owada, T. Shiigai, Accumulation of indoxyl-beta-D-glucuronide in uremic serum: suppression of its production by oral sorbent and efficient removal by hemodialysis, *Nephron* 74 (1996) 72–78.
- [20] S. Agatsuma, H. Sekino, H. Watanabe, Indoxyl-beta-D-glucuronide and 3-indoxyl sulfate in plasma of hemodialysis patients, *Clin. Nephrol.* 45 (1996) 250–256.
- [21] S. Ohno, S. Nakajin, Determination of mRNA expression of human UDP-glucuronosyltransferases and application for localization in various human



- tissues by real-time reverse transcriptase-polymerase chain reaction, *Drug Metab. Dispos.* 37 (2009) 32–40.
- [22] K.W. Bock, Functions and transcriptional regulation of adult human hepatic UDP-glucuronosyl-transferases (UGTs): mechanisms responsible for interindividual variation of UGT levels, *Biochem. Pharmacol.* 80 (2010) 771–777.
- [23] G.G. Gibson, P. Skett, Pathways of drug metabolism, *Introduction to Drug Metabolism*, Second ed., Chapman & Hall, London, 1995.
- [24] L. Braun, T. Kardon, F. Puskas, M. Csala, G. Banhegyi, J. Mandl, Regulation of glucuronidation by glutathione redox state through the alteration of UDP-glucose supply originating from glycogen metabolism, *Arch. Biochem. Biophys.* 348 (1997) 169–173.
- [25] O. Kerdpin, K.M. Knights, D.J. Elliot, J.O. Miners, *In vitro* characterisation of human renal and hepatic frusemide glucuronidation and identification of the UDP-glucuronosyltransferase enzymes involved in this pathway, *Biochem. Pharmacol.* 76 (2008) 249–257.
- [26] C. Yu, J.K. Ritter, R.J. Krieg, B. Rege, T.H. Karnes, M.A. Sarkar, Effect of chronic renal insufficiency on hepatic and renal udp-glucuronyltransferases in rats, *Drug Metab. Dispos.* 34 (2006) 621–627.
- [27] G. Cohen, G. Glorieux, P. Thornalley, E. Schepers, N. Meert, J. Jankowski, V. Jankowski, A. Argiles, B. Anderstam, P. Brunet, C. Cerini, L. Dou, R. Deppisch, B. Marescau, Z. Massy, A. Perna, J. Raupachova, M. Rodriguez, B. Stegmayr, R. Vanholder, W.H. Horl, Review on uraemic toxins III: recommendations for handling uraemic retention solutes *in vitro*—towards a standardized approach for research on uraemia, *Nephrol. Dial. Transplant.* 22 (2007) 3381–3390.
- [28] J. Feigenbaum, C.A. Neuberger, Simplified method for the preparation of aromatic sulfuric acid esters, *J. Am. Chem. Soc.* 63 (1941) 3529–3530.
- [29] E. Van der Eycken, N. Terry, J.L. Goeman, G. Carlens, W. Nerinckx, M. Claeysens, J. Van der Eycken, M. Van Montagu, M. Brito-Arias, G. Engler, Sudan- $\beta$ -D-glucuronidase and their use for the histochemical localization of  $\beta$ -glucuronidase activity in transgenic plants, *Plant Cell Rep.* 19 (2000) 966–970.
- [30] M.J. Wilmer, M.A. Saleem, R. Masereeuw, L. Ni, D. Van, V.F.G. Russel, P.W. Mathieson, L.A. Monnens, L.P. van den Heuvel, E.N. Levchenko, Novel conditionally immortalized human proximal tubule cell line expressing functional influx and efflux transporters, *Cell Tissue Res.* 339 (2009) 449–457.
- [31] H.G.M. Wittgen, J.J.M.W. van den Heuvel, P.H.H. van den Broek, S. Siissalo, G.M.M. Groothuis, I.A.M. de Graaf, J.B. Koenderink, F.G.M. Russel, Transport of the coumarin metabolite 7-hydroxycoumarin glucuronide is mediated via multidrug resistance-associated proteins 3 and 4, *Drug Metab. Dispos.* 40 (2012) 1076–1079.
- [32] E. Hutter, K. Renner, G. Pfister, P. Stockl, P. Jansen-Durr, E. Gnaiger, Senescence-associated changes in respiration and oxidative phosphorylation in primary human fibroblasts, *Biochem. J.* 380 (2004) 919–928.
- [33] H.A. Mutsaers, L.P. van den Heuvel, L.H. Ringens, A.C. Dankers, F.G. Russel, J.F. Wetzels, J.G. Hoenderop, R. Masereeuw, Uremic toxins inhibit transport by breast cancer resistance protein and multidrug resistance protein 4 at clinically relevant concentrations, *PLoS One* 6 (2011) e18438.
- [34] L.H. Lash, D.A. Putt, H. Cai, Drug metabolism enzyme expression and activity in primary cultures of human proximal tubular cells, *Toxicology* 244 (2008) 56–65.
- [35] G.J. Schaaf, E.M. de Groene, R.F. Maas, J.N. Commandeur, J. Fink-Gremmels, Characterization of biotransformation enzyme activities in primary rat proximal tubular cells, *Chem. Biol. Interact.* 134 (2001) 167–190.
- [36] R. Moghadasali, H.A. Mutsaers, M. Azarnia, M. Aghdami, H. Baharvand, R. Torensma, M.J. Wilmer, R. Masereeuw, Mesenchymal stem cell-conditioned medium accelerates regeneration of human renal proximal tubule epithelial cells after gentamicin toxicity, *Exp. Toxicol. Pathol.* (in press), <http://dx.doi.org/10.1016/j.etp.2012.06.002>.
- [37] R. Vanholder, B. Bammens, L.H. de, G. Glorieux, B. Meijers, E. Schepers, Z. Massy, P. Evenepoel, Warning: the unfortunate end of p-cresol as a uraemic toxin, *Nephrol. Dial. Transplant.* 26 (2011) 1464–1467.
- [38] P. Wang, S.M. Henning, D. Heber, Limitations of MTT and MTS-based assays for measurement of antiproliferative activity of green tea polyphenols, *PLoS One* 5 (2010) e10202.
- [39] C.R. Lancaster, Succinate:quinone oxidoreductases: an overview, *Biochim. Biophys. Acta* 1553 (2002) 1–6.
- [40] H. Massudi, R. Grant, G.J. Guillemin, N. Braid, NAD<sup>+</sup> metabolism and oxidative stress: the golden nucleotide on a crown of thorns, *Redox Rep.* 17 (2012) 28–46.
- [41] T.W. Stone, L.G. Darlington, Endogenous kynurenes as targets for drug discovery and development, *Nat. Rev. Drug Discov.* 1 (2002) 609–620.
- [42] E.P. Rhee, A. Souza, L. Farrell, M.R. Pollak, G.D. Lewis, D.J. Steele, R. Thadhani, C.B. Clish, A. Greka, R.E. Gerszten, Metabolite profiling identifies markers of uremia, *J. Am. Soc. Nephrol.* 21 (2010) 1041–1051.
- [43] T. Fukuwatari, Y. Morikawa, F. Hayakawa, E. Sugimoto, K. Shibata, Influence of adenine-induced renal failure on tryptophan-niacin metabolism in rats, *Biosci. Biotechnol. Biochem.* 65 (2001) 2154–2161.
- [44] S. Owada, T. Maeba, Y. Sugano, A. Hirayama, A. Ueda, S. Nagase, S. Goto, F. Nishijima, K. Bannai, H. Yamato, Spherical carbon adsorbent (AST-120) protects deterioration of renal function in chronic kidney disease rats through inhibition of reactive oxygen species production from mitochondria and reduction of serum lipid peroxidation, *Nephron Exp. Nephrol.* 115 (2010) e101–e111.
- [45] R. Dzurik, V. Spustova, Z. Krivosikova, K. Gazdikova, Hippurate participates in the correction of metabolic acidosis, *Kidney Int. Suppl.* 78 (2001) S278–S281.
- [46] A. Kitagawa, Effects of cresols (o-, m-, and p-isomers) on the bioenergetic system in isolated rat liver mitochondria, *Drug Chem. Toxicol.* 24 (2001) 39–47.
- [47] W. Riegel, C. Ulrich, S. Sauerneheimer, R.M. Deppisch, H. Kohler, Hepatotoxic substance(s) removed by high-flux membranes enhances the positive acute phase response, *Kidney Int. Suppl.* 78 (2001) S308–S314.
- [48] R. Vanholder, S.R. De, G. Glorieux, A. Argiles, U. Baurmeister, P. Brunet, W. Clark, G. Cohen, P.P. De Deyn, R. Deppisch, B. Scamps-Latscha, T. Henle, A. Jorres, H.D. Lemke, Z.A. Massy, J. Passlick-Deetjen, M. Rodriguez, B. Stegmayr, P. Stenvinkel, C. Tetta, C. Wanner, W. Zidek, Review on uremic toxins: classification, concentration, and interindividual variability, *Kidney Int.* 63 (2003) 1934–1943.
- [49] J. Jankowski, G.M. van der, V. Jankowski, S. Schmidt, M. Hemeier, B. Mahn, G. Giebing, M. Tolle, H. Luftmann, H. Schluter, W. Zidek, H. Tepel, Increased plasma phenylacetic acid in patients with end-stage renal failure inhibits iNOS expression, *J. Clin. Invest.* 112 (2003) 256–264.
- [50] F. Duranton, G. Cohen, S.R. De, M. Rodriguez, J. Jankowski, R. Vanholder, A. Argiles, Normal and pathologic concentrations of uremic toxins, *J. Am. Soc. Nephrol.* 23 (2012) 1258–1270.
- [51] T. Deguchi, S. Ohtsuki, M. Otagiri, H. Takanaga, H. Asaba, S. Mori, T. Terasaki, Major role of organic anion transporter 3 in the transport of indoxyl sulfate in the kidney, *Kidney Int.* 61 (2002) 1760–1768.
- [52] T. Deguchi, H. Kusuhara, A. Takadate, H. Endou, M. Otagiri, Y. Sugiyama, Characterization of uremic toxin transport by organic anion transporters in the kidney, *Kidney Int.* 65 (2004) 162–174.
- [53] T. Toyohara, T. Suzuki, R. Morimoto, Y. Akiyama, T. Souma, H.O. Shiwaku, Y. Takeuchi, E. Mishima, M. Abe, M. Tanemoto, S. Masuda, H. Kawano, K. Maemura, M. Nakayama, H. Sato, T. Mikkaichi, H. Yamaguchi, S. Fukui, Y. Fukumoto, H. Shimokawa, K. Inui, T. Terasaki, J. Goto, S. Ito, T. Hishinuma, I. Rubera, M. Tauc, Y. Fujii-Kuriyama, H. Yabuuchi, Y. Moriyama, T. Soga, T. Abe, SLC04C1 transporter eliminates uremic toxins and attenuates hypertension and renal inflammation, *J. Am. Soc. Nephrol.* 20 (2009) 2546–2555.
- [54] H.A. Mutsaers, M.J. Wilmer, L.P. van den Heuvel, J.G. Hoenderop, R. Masereeuw, Basolateral transport of the uraemic toxin p-cresyl sulfate: role for organic anion transporters? *Nephrol. Dial. Transplant.* 26 (2011) 4149.
- [55] A. Saito, R. Nagai, A. Tanuma, H. Hama, K. Cho, T. Takeda, Y. Yoshida, T. Toda, F. Shimizu, S. Horiuchi, F. Gejyo, Role of megalin in endocytosis of advanced glycation end products: implications for a novel protein binding to both megalin and advanced glycation end products, *J. Am. Soc. Nephrol.* 14 (2003) 1123–1131.
- [56] R. Masereeuw, M.M. Moons, F.G. Russel, Renal excretion and accumulation kinetics of 2-methylbenzoylglycine in the isolated perfused rat kidney, *J. Pharm. Pharmacol.* 48 (1996) 560–565.
- [57] R. Masereeuw, M.M. Moons, F.G. Russel, Disposition of 4-methylbenzoylglycine in rat isolated perfused kidney and effects of hippurates on renal mitochondrial metabolism, *J. Pharm. Pharmacol.* 50 (1998) 1397–1404.
- [58] F.A. Leblond, L. Giroux, J.P. Villeneuve, V. Pichette, Decreased *in vivo* metabolism of drugs in chronic renal failure, *Drug Metab. Dispos.* 28 (2000) 1317–1320.
- [59] F. Leblond, C. Guevin, C. Demers, I. Pellerin, M. Gascon-Barre, V. Pichette, Downregulation of hepatic cytochrome P450 in chronic renal failure, *J. Am. Soc. Nephrol.* 12 (2001) 326–332.
- [60] J. Naud, J. Michaud, S. Beauchemin, M.J. Hebert, M. Roger, S. Lefrancois, F.A. Leblond, V. Pichette, Effects of chronic renal failure on kidney drug transporters and cytochrome P450 in rats, *Drug Metab. Dispos.* 39 (2011) 1363–1369.
- [61] H. Sun, Y. Huang, L. Frassetto, L.Z. Benet, Effects of uremic toxins on hepatic uptake and metabolism of erythromycin, *Drug Metab. Dispos.* 32 (2004) 1239–1246.
- [62] Z.H. Huang, T. Murakami, A. Okochi, R. Yumoto, J. Nagai, M. Takano, Expression and function of P-glycoprotein in rats with glycerol-induced acute renal failure, *Eur. J. Pharmacol.* 406 (2000) 453–460.
- [63] K.M. Knights, J.O. Miners, Renal UDP-glucuronosyltransferases and the glucuronidation of xenobiotics and endogenous mediators, *Drug Metab. Rev.* 42 (2010) 63–73.